applied sciences

IMPACT FACTOR 2.5

CITESCORE 5.3

Article

Development of the Viscous Plane Damper Applicable in Limited Space within Structures Subjected to Dynamic Loads

Mohd Ridzuan Bin Mohd Ali and Farzad Hejazi

Special Issue
Advances in Architectural Acoustics and Vibration

Edited by
Dr. Sanjay Kumar

MDPI

https://doi.org/10.3390/app14199029

applied sciences

MDPI

Article

Development of the Viscous Plane Damper Applicable in Limited Space within Structures Subjected to Dynamic Loads

Mohd Ridzuan Bin Mohd Ali [1,2] and Farzad Hejazi [3,*]

[1] Department of Civil Engineering, University Putra Malaysia, Serdang 43400, Malaysia; ridzuan1995@salam.uitm.edu.my
[2] Department of Civil Engineering, Universiti Teknologi MARA, Shah Alam 40450, Malaysia
[3] Faculty of Environment and Technology, The University of The West England, Bristol BS16 1QY, UK
* Correspondence: farzad.hejazi@uwe.ac.uk

Abstract: Shipping impact and wave loads impose dynamic loads on jetties and platforms in the sea, which cause the vibration of structures. Recently, many advanced viscous damper devices have been developed for implementation in structures to diminish structural vibration due to earthquakes or wind. However, the longitudinal configuration of conventional viscous damper devices requires adequate space to locate the damper device within the frame structure, which limits the application of viscous dampers for use in jetties or platforms to dissipate the vibrations imposed by ship impact or wave force. For this reason, in this study, an attempt has been made to develop a new viscous plane damper device applicable in limited space positions where the longitudinal damper device is not able to fit. For this purpose, the initial design for the viscous plane damper device is proposed, and the prototype of the device is manufactured. Then, the performance of the fabricated viscous plane damper is examined through experimental tests by applying cyclic loads using a dynamic actuator. In order to investigate the effect of the diameter and configuration of the piston's orifices, five different diameters for the orifices of 1, 2, 5, 8, and 10 mm are included, and three different distribution configurations of the orifices in the piston plate as Configurations A, B, and C are manufactured and tested experimentally. The lab testing is conducted by applying cyclic loads with different frequencies to evaluate the performance of the developed plane damper device under various load velocities. Accordingly, the dynamic performance of the damper device, including the damping force, effective damping and stiffness and the energy dissipation capacity obtained from the hysteresis response (force–displacement result), is investigated. The results of the experimental tests prove the functionality of the developed device to generate the desired damping force and vibration energy dissipation during applied cyclic loads. Therefore, the new plane damper device can be implemented in any structure to dissipate the effect of imposed vibration.

Keywords: structural control device; dampers; viscous damper; retrofitting; earthquake; cyclic load; impact load

Citation: Bin Mohd Ali, M.R.; Hejazi, F. Development of the Viscous Plane Damper Applicable in Limited Space within Structures Subjected to Dynamic Loads. *Appl. Sci.* **2024**, *14*, 9029. https://doi.org/10.3390/app14199029

Academic Editor: Sanjay Kumar

Received: 1 September 2024
Revised: 27 September 2024
Accepted: 30 September 2024
Published: 6 October 2024

1. Introduction

In recent years, many different innovative types of damping systems have been developed, such as Sliding LRBs [1], superelastic pendulum isolators [2], and passive adaptive isolation bearings (PAIBs) [3] all manufactured by Southeast University in Nanjing, China, which demonstrate high performance in successfully dissipating applied vibrations in structures. However, these systems are applicable only in newly designed structures, and their practical use is not common. Additionally, these devices do not require much space for installation, but they are not suitable for areas with limited space.

In recent years, significant strides have been made in the development of viscous damper technology and damping systems to enhance the safety and efficiency of structures under seismic conditions. Various techniques have been employed for the seismic

retrofitting of buildings, with the installation of supplementary damper devices being one of the most effective methods. Ahsan Kareem, Tracy Kijewski, and Yukio Tamura (1999) emphasized the role of such dampers in dissipating structural vibrations, thereby enhancing the integrity and stability of buildings [4]. Consequently, numerous studies have explored the implementation of dampers to reduce displacement and increase seismic performance [5].

The exposure of structures to severe deformations due to external forces, like earthquakes, tsunamis, or strong winds, can cause substantial damage. Petti and De Iuliis (2008) asserted that structural components often suffer damage due to the horizontal or rotational movement of buildings under such conditions [6]. F. Hejazi et al. (2011) studied the vulnerability of multi-story reinforced-concrete buildings during earthquakes, particularly focusing on the effect of soft stories, where reduced lateral stiffness leads to structural failure. They found that adding bracing to the lower levels significantly improves seismic performance by enhancing lateral strength and reducing displacement. The research highlights that the placement and configuration of bracing are crucial in mitigating the soft story effect, thus providing effective retrofitting strategies for existing buildings to meet safety requirements and minimize earthquake damage [7].

Rouhani et al. (2024) **explored** the dynamic performance of a novel tackle-damper configuration, which **combined** a viscous damper with two inclined tackles made of wire ropes. This setup **enhanced** the damper deformations and forces, **shifting** the damper's behavior from purely viscous to viscoelastic. Their experiments **revealed** that energy dissipation **occurred** from both the viscous damper and capstan friction, leading to the significant amplification of forces and energy. Deformation amplification factors **ranged** from 0.29 to 1.9, while force amplification factors **reached** between 5.3 and 58. The study **emphasized** that friction and wire rope elongation **could significantly affect** the actual amplification capabilities, suggesting that optimized designs **were necessary** to achieve ideal performance levels. However, this device **was not applicable** to limited spaces [8].

The evolution of fluid viscous dampers (FVDs) from passive systems to more sophisticated semi-active and adaptive systems has been a focus of recent research. Zoccolini et al. (2023) demonstrated that semi-active and adaptive dampers provide superior performance across different seismic intensities, although these advancements come with increased complexity and costs [9].

Zhou et al. (2022) investigated the seismic response of multi-story buildings equipped with FVDs, focusing on energy perspectives. Their research found that increasing the additional damping ratio (ξ_add) generally reduces structural plastic energy and enhances the energy dissipated by dampers, although values above 20% show diminishing returns [10]. Furthermore, dampers with a velocity power α of 0.3 are not suitable for tall buildings. Zhou and colleagues also introduced a three-stage variable-damping-coefficient viscous fluid damper (VCVFD) tailored for high-intensity earthquakes, which significantly increased the structural damping ratios and reduced displacement under strong seismic loads [11].

Exploring numerical models for FVDs, Cucuzza et al. (2023) identified that differential models typically offer greater accuracy compared to algebraic ones. Notably, models Law#8 and Law#9 demonstrated both high accuracy and robustness, while Law#2, though robust, had lower precision [12]. Shang et al. (2023) introduced a novel viscous damping wall (VDW) featuring a displacement amplification mechanism, which outperformed traditional VDWs in reducing structural acceleration, inter-story displacement, and shear forces [13].

Tang et al. (2021) **discussed** the evolution of passive energy dissipation systems, particularly viscous fluid dampers, designed to enhance seismic performance in structures. These dampers **convert** kinetic energy into heat, effectively absorbing seismic energy and allowing structures to remain undamaged post-earthquake. Their full-scale experiments **demonstrated** stable mechanical properties, with hysteresis loops **resembling** a rectangular shape, indicating strong energy dissipation capability. The results **showed** damping force measurements within 15% of the design values, smooth hysteresis curves, and no leakage or

permanent deformation, confirming the reliability of these dampers in seismic applications. In the context of reinforced concrete structures [14], Faruk et al. (2023) compared the performance of buckling-restrained braces (BRBs) and FVDs. Their findings revealed that BRBs are more effective in enhancing overall stiffness and structural capacity, whereas FVDs are superior in handling large displacements [15]. Parajuli et al. (2023) investigated the impact of various FVD configurations and damping coefficient distribution methods in ten-story moment-resisting buildings. Their study showed that damper configuration plays a crucial role in seismic performance, while the method of distribution has a lesser impact [16].

Further examining the effects of damper parameters, Lan et al. (2024) utilized a response surface method to model damping efficiency in frame shear wall structures, demonstrating higher accuracy and predictability over traditional sensitivity analyses [17]. Lan and colleagues also conducted shaking table tests on two-story steel structures, highlighting that dampers positioned at the mid-span effectively reduced vertex displacement and base shear [18].

Yang et al. (2024) introduced the Asynchronized Parallel Double-Stage Viscous Fluid Damper (APDVFD), which adapts its performance based on deformation levels. Their full-scale tests confirmed the effectiveness of APDVFD in managing high response control under extreme conditions with minimal fatigue loss [19]. He et al. (2022) proposed a Multilayer Viscous Damping Wall with Amplified Deformation (MADW), showing significantly increased damping forces and energy dissipation, particularly during severe earthquakes [20].

Hu et al. (2024) **developed** a hybrid self-centering brace (HSB) to improve seismic resilience in buildings by controlling both structural and nonstructural damage. The HSB **combines** NiTi-based shape memory alloy dampers for self-centering and viscoelastic dampers for velocity-proportional damping. Their study **demonstrated** that the HSB effectively **reduced** deformations, base shear, and residual accelerations, showcasing its potential for enhancing earthquake-resistant structures [21].

Farahpour and Hejazi (2023) developed a Semi-Active Bypass Fluid Damper (SABFD) for bridge vibration control, employing programmable logic controllers (PLCs) and fuzzy control algorithms [22]. This innovation significantly reduced bridge displacements and improved structural responses under traffic-induced vibrations. Hejazi et al. (2024) introduced a rubber bracing damper (RBD) system using high-damping rubber to dissipate energy, which was shown to reduce lateral displacements and prevent the formation of plastic hinges, enhancing seismic performance by up to 69% [23].

The advancements in damper technology reflect a growing interest in developing systems capable of effectively managing seismic loads driven by the increasing frequency of earthquakes and other natural hazards [24]. Different types of dampers, such as Tuned Mass Dampers (TMDs), tuned liquid dampers (TLDs), and Tuned Liquid Column Dampers (TLCDs), have been explored for maintaining and retrofitting structures [25]. As these studies indicate, the evolution and refinement of damper systems continue to play a vital role in safeguarding structures against seismic forces and improving overall resilience.

Viscous dampers (VDs) are a form of base isolation commonly used to dissipate energy and enhance the damping ratio of structures, ensuring their stability and safety. Love and Tait (2012) noted that examples of liquid dampers include tuned liquid dampers (TLDs) and Tuned Liquid Column Dampers (TLCDs). In contrast, VDs are a type of Dynamic Vibration Absorber (DVA) that is simple and easy to manage [26]. Viscous dampers are particularly beneficial for buildings due to their low maintenance requirements and cost-effectiveness [25], as well as their practical application. The rapid advancement of damper technology highlights the significant impact these devices have in addressing issues related to the strength and stability of buildings.

VDs are utilized in various applications, including vehicle suspensions, high-rise buildings, bridge supports, and machinery suspensions. According to Silwal et al. (2015), VDs can dissipate energy in buildings at different levels of vibration while simultaneously

maintaining stiffness. Buildings and structures that endure disasters typically require repair and retrofitting. VDs are a preferred option for such strengthening and retrofitting work due to their compact size and ease of installation [27].

Hao Su et al. (2024) investigated the open-space viscous damper installation configuration (OSVDIC) that balances structural and architectural needs. Their shaking table tests on a three-story steel-frame model showed that OSVDIC significantly reduced seismic responses and effectively dissipated energy during earthquakes. The study confirmed the model's accuracy and highlighted OSVDIC's potential to meet damping requirements while addressing aesthetic and functional considerations [28].

Installing viscous dampers (VDs) is challenging in terms of space and area since these components are longitudinal and not applicable for limited space, particularly in existing buildings. However, VDs have the advantage of dissipating loads from multiple directions, making them effective in various seismic scenarios. The movement of structures is influenced by the loads applied, and ground motion due to seismic activity provides a good example of this. When a building experiences ground movement, it may eventually reach a point where its displacement exceeds the design limitations, causing the structure to show signs of weakness and fatigue. At this stage, the building may be at risk of collapse. Structural failures can be attributed to several factors, including earthquakes, design limitations, and defects or damage to elements due to building vibration [29]. Therefore, the type and amount of load that a building may encounter should be carefully considered during the design phase to prevent collapse. Recent designs of VDs have been optimized for installation in constrained spaces.

The piston plate in a VD has an orifice that allows viscous fluid to flow between compartments, affecting the movement of the piston plate. The fluid used is typically incompressible, which means it does not compress easily. As the piston plate moves, the fluid within the barrel begins to move, generating compressive force. The movement of the piston plate changes the volume of viscous fluid in one compartment. Smaller compartments generate higher force compared to larger ones. Ras and Boumechra (2016) found that the speed of the piston plate's movement is directly related to the force generated. Additionally, the fluid's viscosity and the orifice diameter affect the force output. Generally, when supplementary viscous dampers are installed in a frame, they can reduce movement from the bottom floor by 4% and up to 32% for the top floor [30].

The frequency of natural disasters, such as earthquakes, tsunamis, and tornadoes, has increased annually. These events can have significant impacts on buildings and structures. Buildings unable to withstand seismic tremors may collapse due to excessive movement. Failures in building design have driven advancements in more resilient building technologies, which is a growing area of research. A key failure factor is the collapse of building structures when they are subjected to loads beyond their design capacity, leading to excessive movement. In such conditions, structural components may fail to control deformation and dissipate energy effectively, leading to exhaustion of the structure, especially at the joints between components.

VDs are easier to install than many other types of dampers due to their relatively small size. Martinez-Rodrigo and Romero (2003) demonstrated that viscous dampers do not require a large installation area, making them suitable for retrofitting existing buildings without major difficulty. However, installing dampers in existing buildings can be challenging because strengthening and retrofitting often involves installing new, larger, and heavier dampers than the original ones. Increased damper dimensions may not fit in the same space, necessitating significant repairs for installation. For offshore structures with rounded components, damper installation is also costly because it requires specialized skills and equipment [31].

The installation area required for tuned liquid dampers (TLDs) is dependent on the dimensions of the water tank and its working area. Larger tanks can dissipate more energy, but they also require more space. In existing structures, space is often limited, making it difficult to install new TLDs after seismic events due to the increased tank size

and lack of available space. Finding suitable space in existing structures may require additional modifications.

The scenario, however, differs at jetties, yards, and ports. These buildings must be capable of withstanding the substantial impact forces exerted by large vessels. Given the high levels of energy they encounter, the dampers in these structures need to have a high capacity to absorb these impacts. To achieve a high-capacity damper, its size must be large, which poses challenges for installation due to limited working areas and the damper's unwieldy size. The ideal location for installing a conventional VD would be under the floor near the seawater surface. However, this positioning necessitates regular maintenance due to exposure to harsh marine conditions.

The integrity of offshore structures is heavily influenced by design considerations for environmental loads such as wind, waves, and earthquakes. These structures must be able to withstand high-magnitude loads with return periods of 50 or 100 years. According to studies by Jin et al. (2007), the addition of damping devices can significantly enhance the stability of offshore structures. These studies demonstrated that oscillatory motions induced by vibrations present a significant load, and the use of tuned liquid dampers showed promising results. Testing revealed the effectiveness of these dampers based on their mass ratio, which helps to improve the damping ratio and reduce structural vibrations. However, a drawback is that these dampers are not cost-effective. The authors found that the mass ratio of the dampers ranged from 1% to 5% [32].

The configuration and arrangement of conventional viscous dampers are ©mpractical for installation in areas with limited space, such as those found in these structures. Even new buildings may encounter similar issues if space for damper installation is not incorporated into the design phase.

Therefore, this study reports on the development of a new viscous plane damper specifically designed for cyclic loads. Experimental testing was conducted using a dynamic actuator to simulate different load frequencies. Additionally, the effects of orifice diameters and the configuration of the piston's location within the device were evaluated through these experimental tests.

2. Designing the Device

In this research work, an attempt was made to develop a novel viscous plane damping device in Structural Lab, University Putra Malaysia (Serdang, Malaysia) for use in structures which have limited space for installing conventional viscous damper systems. Accordingly, the novel design detail for the viscous plane damper was developed, the prototype of the device was manufactured, and experimental tests using a dynamic actuator were employed to assess the performance of the proposed viscous plane damper.

3. Detailed Design of Viscous Plane Damper

The newly proposed viscous plane damper is square-shaped and consists of a box barrel (cylindrical), piston plate, piston rod, head mounting, and bottom mounting. The key difference between typical viscous dampers and the new viscous plane damper lies in the shape of the piston plate and box barrel, which has been changed from the conventional circular form to a square shape. Additionally, the cross-sectional area of the damper device and the configuration of the orifices on the piston plate have been redesigned to achieve the desired performance and functionality. Figure 1 illustrates the detailed configurations of both a conventional viscous damper and the newly developed viscous plane damper used in this study.

The new viscous plane damper is designed with simple components to facilitate easy manufacturing and installation, particularly in limited-space areas. The damper's components are also separate to ensure easy handling and transportation. Upon installation, these components can be easily assembled to form the complete viscous plane damper.

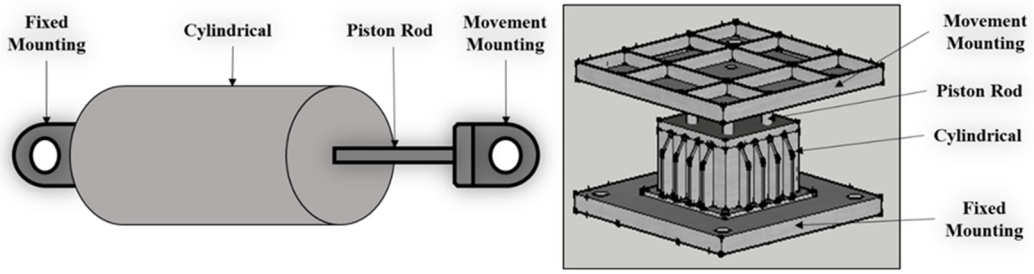

(**a**) Typical Viscous Damper (**b**) Viscous Plane Damper

Figure 1. Configuration of conventional viscous damper and proposed viscous plane damper.

The most crucial component of the viscous plane damper is the piston plate, which is square-shaped and features tiny holes serving as orifices. These orifices generally allow the viscous fluid to transfer from one side to the other. In this study, different configurations and various orifice diameters were explored to optimize the damper's performance. The positioning of the orifices on the piston plate is shown in Figure 2. Three distinct configurations were tested, labeled A, B, and C. Configuration A has 16 holes arranged in a 4×4 matrix. Configurations B and C each have 4 holes but with different arrangements and positions on the piston plate. Configuration A serves as the control sample, providing a baseline prediction of fluid flow behavior.

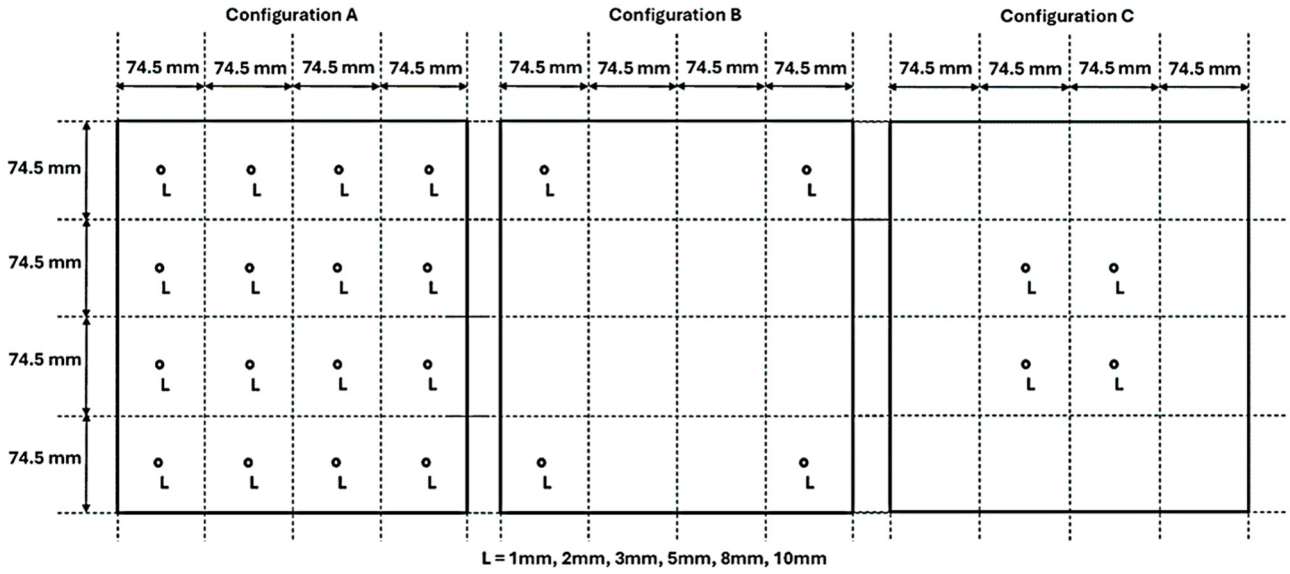

Figure 2. Configuration of the orifices on the piston plate.

Additionally, each configuration was evaluated with four different orifice diameters, 1 mm, 2 mm, 5 mm, and 10 mm, to assess the impact of orifice diameter on pressure drop and the performance of the viscous plane damper.

As shown in Table 1, the total cross-sectional open area of the orifices in Configuration A is four times larger than that in Configurations B and C. Consequently, the total open area in Configurations B and C is only 25% of that in Configuration A. Furthermore, the total open area of a 10 mm diameter orifice is four times greater than that of a 5 mm diameter orifice across all configurations. The total cross-sectional open area for a 5 mm diameter orifice in Configuration A is nearly equivalent to that of Configurations B and C. Overall, various orifice diameters were analyzed to determine the behavior of the viscous fluid as it flowed through the orifices and evaluate the effect of pressure drop on the damping force and damping ratio.

Table 1. Total cross-sectional open area of orifice on the piston plate.

Diameter (mm)	Area per Hole (mm^2)	Configuration		
		A	B	C
		Total Area (mm^2)		
1	0.79	12.57	3.14	3.14
2	3.14	50.27	12.57	12.57
5	19.64	314.20	78.55	78.55
10	78.55	1256.80	314.20	314.20

The schematic drawing of the developed viscous plane damper is presented in Figure 3. As shown in the figure, the new viscous plane damper features a distinct shape and dimensions. The length or height of the viscous plane damper is shorter compared to that of a typical viscous damper, making it suitable for installation in confined spaces. Additionally, the new viscous plane damper is wider than the diameter of a conventional viscous damper, providing an adequate area for the cylinder cube to generate pressure drop and damping force.

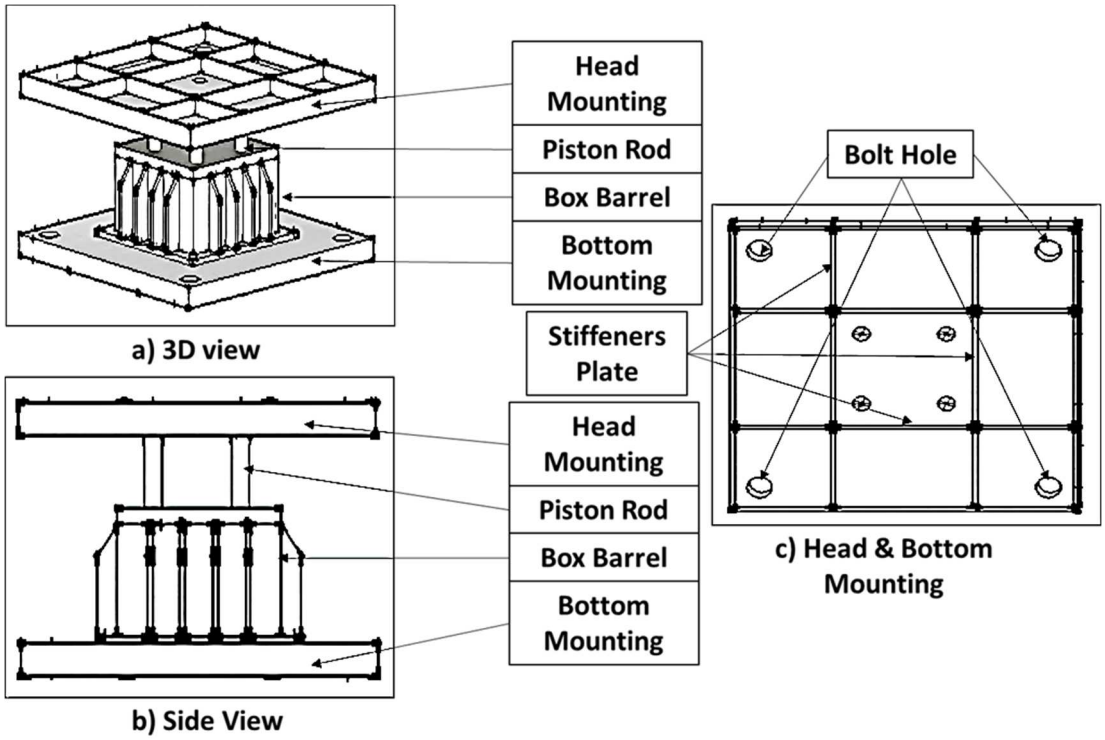

Figure 3. Section view of viscous plane damper.

The new design of the viscous plane damper consists of separate components: head mounting, box barrel, piston rod, piston plate, and bottom mounting. The mountings are used to attach the damper to the structural elements. The piston plate and piston rod are installed inside the box barrel. The barrel is secured to the bottom mounting with bolts and nuts. Additionally, the piston rod connects the piston plate to the head mounting. The mountings are designed to move parallel to the structural movement.

To ensure that the mountings and box barrel can withstand significant external forces, stiffener plates were welded to these components to prevent bending and breaking.

The prototype of the viscous plane damper was fabricated in separate parts, which were then assembled to form the complete damper, as illustrated in Figure 4. Handling and

installing the loose parts is practical and convenient. The names of the parts are labeled in Figure 4.

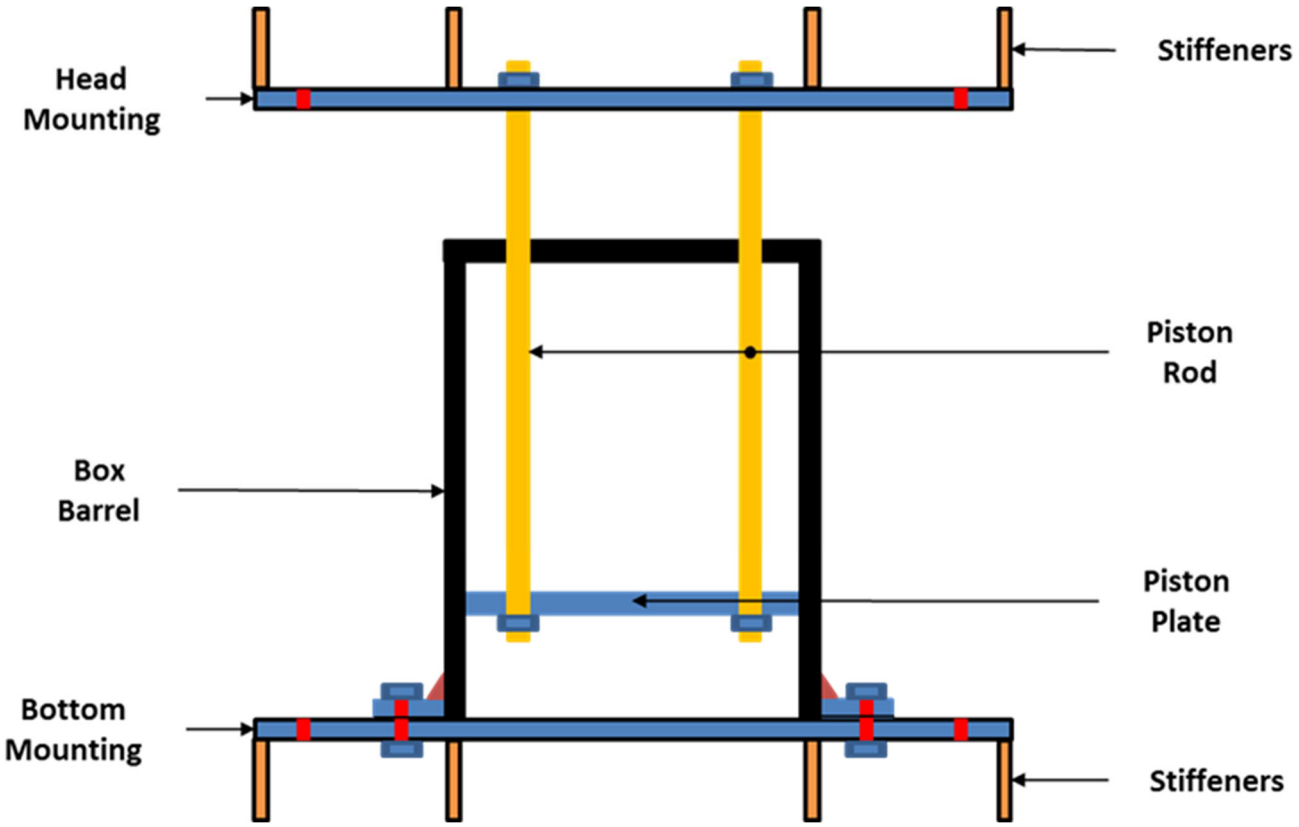

Figure 4. Elevation section of the viscous plane damper.

Figure 5 illustrates the detailed schematic drawing of the dimensions for the viscous plane damper. The dimensions of the newly designed viscous plane damper are 0.3 m in width, 0.3 m in length, and 0.15 m in height. The detailed dimensions of the damper are shown in Figure 5.

3.1. Viscosity of Fluid Liquid

It is also important to note that the effectiveness of a viscous damper in reducing structural movement depends on the drop pressure created by the flow of viscous oil through the orifices during piston movement within the box barrel. Therefore, ensuring that the fluid within the box barrel has the appropriate viscosity is crucial for generating the desired drop pressure. The characteristics of the fluid significantly impact the performance of the viscous plane damper. Table 2 presents the properties of the liquid used in this study. An incompressible fluid was selected to ensure that the fluid volume in the box barrel remains constant despite piston plate movement.

3.2. Theory of Viscous Plane Dampers Using Orifices

The proposed viscous plane damper is designed to create a pressure differential across a piston, using a small orifice to force fluid through, which generates a damping force. Energy dissipation occurs due to the resistance encountered by the fluid as it moves through these orifices, which leads to a pressure drop and converts mechanical energy into heat. Therefore, in the developed viscous plane damper, the fundamental mechanism involves the movement of fluid (oil or another viscous liquid) through small orifices as the piston moves within a sealed cylinder. The damping force arises from the pressure differential generated by the fluid being forced through these orifices. The Key Theoretical Concepts are demonstrated as follows:

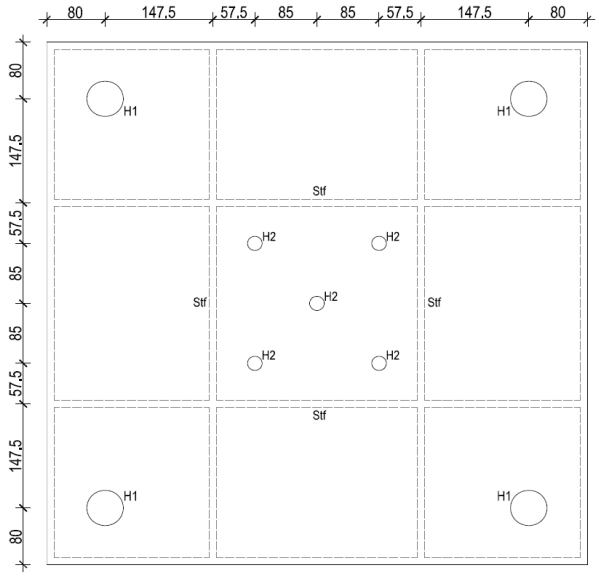

Heading mounting (700 mm × 700 mm × 10 mm Thk)

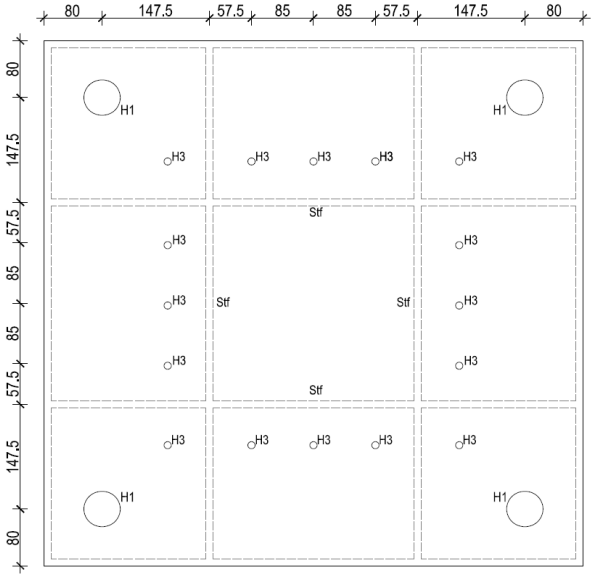

Bottom mounting (700 mm × 700 mm × 10 mm Thk)

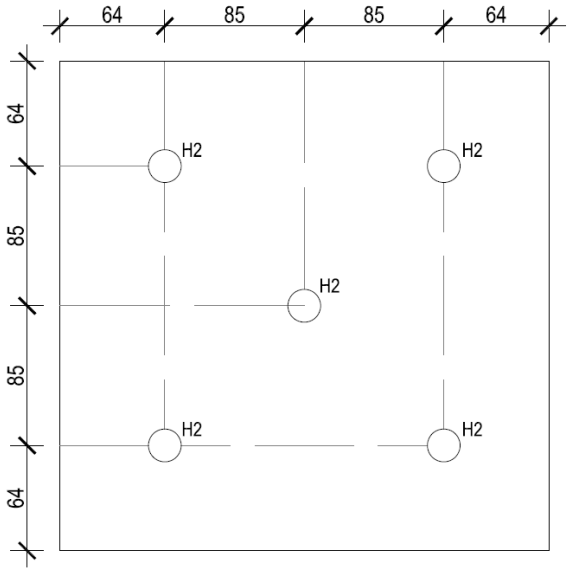

Piston Plate (298 mm × 298 mm Thk)

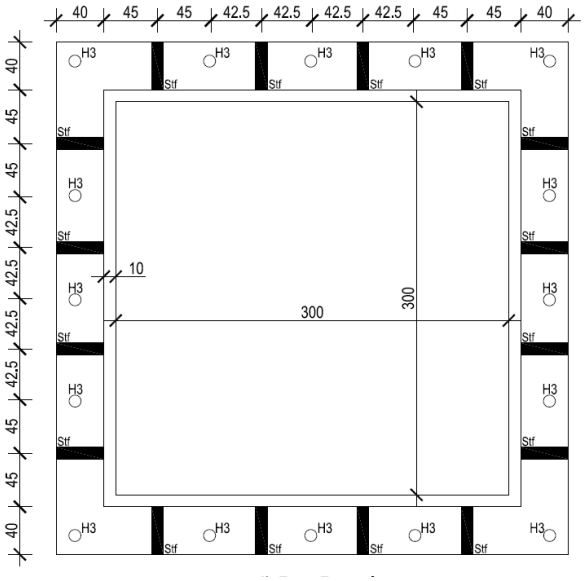

Box Barrel

LABEL	DIAMETER (mm)
H1	50
H2	20
H3	10
Stf	10 (thk)

Table labelling

Figure 5. Detailed drawing of parts of viscous plane damper.

Table 2. Liquid properties.

Description	Detail
Density at 15 C (kg/m^3)	888
Air Release at 50 C (min)	1.1
Flash Point (C)	216
FZG Fail Load Stage	12
Pour Point (C)	−33
Oxidation Stability (TOST), (h)	5000+
Viscosity:	
At 40 C (mm^2/s)	31
At 100 C (mm^2/s)	5.4
Viscosity Index	110

Fluid Dynamics and Pressure Drop: The primary theory governing viscous plane damper is based on fluid mechanics, particularly the principles of Bernoulli's equation and orifice flow. As the piston inside the damper moves, it pushes fluid through small orifices, causing a pressure drop between the two sides of the piston

The relationship between the pressure drop (ΔP) and the fluid flow rate (Q) through an orifice is nonlinear, typically governed by the orifice equation:

$$\Delta P = K \times \frac{Q^2}{A^2}$$

where

ΔP is the pressure differential across the orifice;
K is a constant depending on fluid properties and orifice characteristics;
Q is the volumetric flow rate of the fluid; and
A is the cross-sectional area of the orifice.

3.2.1. Generation of Damping Force

The damping force is created as the piston moves, forcing fluid through the orifices. The force F_d is proportional to the resistance encountered by the fluid. For laminar flow, this force can be approximated as:

$$F_d = C \times \dot{x}$$

where C is a damping coefficient that depends on the orifice size and fluid properties, and $\dot{x}$ is the velocity of the piston.

In reality, for higher flow rates, the flow may become turbulent, and the damping force becomes nonlinear (proportional to $\dot{x}^2$).

3.2.2. Energy Dissipation

As the fluid moves through the orifice, viscous friction causes energy dissipation. The kinetic energy from the vibrations is transformed into heat due to the internal friction in the fluid and the turbulent flow within the damper. This energy dissipation reduces the amplitude of the oscillations, effectively damping the vibrations.

The energy dissipated per cycle of motion is proportional to the area enclosed by the force–displacement loop in the damper's hysteresis curve, indicating the total energy lost.

3.2.3. Orifice Flow and Turbulence

For small velocities, fluid flow through the orifice remains laminar, and the damping force is proportional to velocity (linear damping). As velocities increase, flow may transition to become turbulent, causing a quadratic relationship between the damping force and velocity (nonlinear damping).

3.2.4. Thermodynamic Aspect

The damper operates under the principle of energy conservation, where the mechanical energy from the vibrating system is conserved as heat energy in the fluid. This heat is eventually dissipated through the damper's casing.

3.3. Fabrication of Viscous Plane Damper Prototype

The prototype of the viscous plane damper was manufactured according to the proposed design specifications. Figure 6 shows Prototype 1 of the viscous plane damper, which exhibited inadequate welding quality and an 8 mm steel plate thickness. Following experimental testing, Prototype 1 failed to withstand the pressure within the box barrel due to the viscous fluid leaking through micro-cracks caused by poor welding. Additionally, high pressure within the box barrel contributed to fluid leakage around the surface of the piston rods. To address these issues, an oil ring was incorporated to prevent the viscous fluid from transferring between the two plates and the rounded surface of the piston rod. The second prototype was subsequently manufactured and addressed the leakage issues observed in the first prototype. The new prototype demonstrated improved performance, successfully resolving the leakage problems encountered with the initial design.

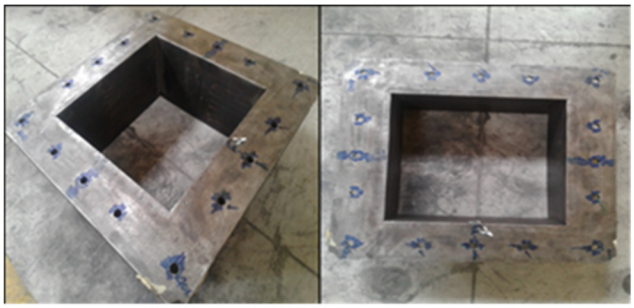

a) Top view inside the box barrel

b) Quality of welding

Figure 6. Prototype 1 of viscous plane damper.

The final prototype of the viscous plane damper was produced with no defects or leakage issues. Improvements were made to address the problems encountered in earlier prototypes. These enhancements included increasing the thickness of the box barrel plates, adding stiffeners, and improving the welding quality. The welding quality was enhanced to prevent leakage due to high pressure inside the barrel, and stiffener plates were welded to the external wall of the box barrel to provide additional support.

The internal surface of the box barrel was smoothed to reduce friction and facilitate smoother movement of the piston plate within the barrel. Additionally, the piston rod was sanded to remove any scratches. Figure 7 shows the final prototype of the viscous plane damper, reflecting these improvements.

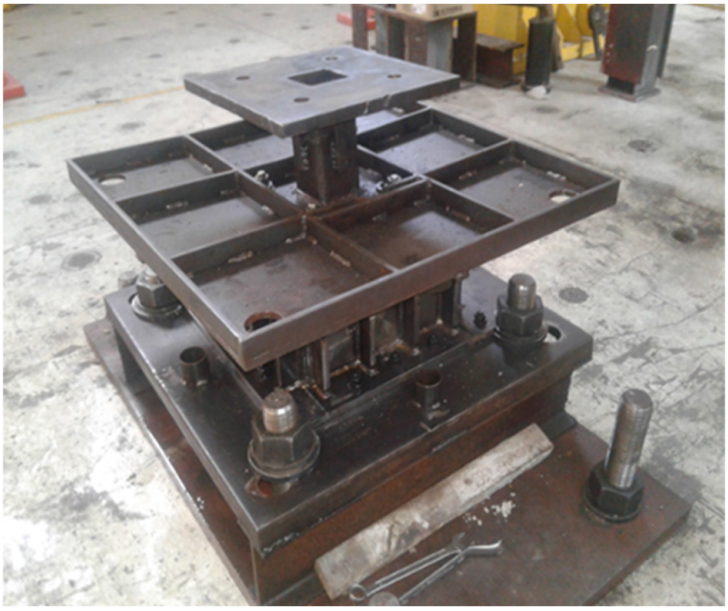

Figure 7. Final prototype of viscous plane damper.

One notable feature of the new viscous plane damper is its ease of transportation and assembly. The design of the damper includes separate components that are straightforward to assemble on-site and fill with oil. The assembly process for the viscous plane damper is outlined as follows:

Figure 8 illustrates the bottom mounting of the main component of the viscous plane damper. The bottom mounting is installed on top of the base plate and secured using four main anchoring bolts. Similarly, the base plate is positioned on a robust floor and fixed with four anchoring bolts.

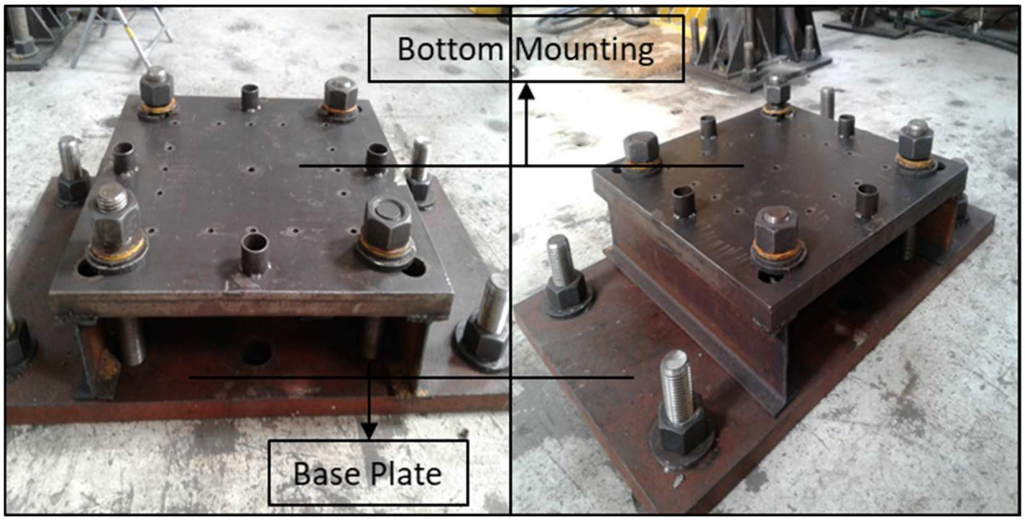

Figure 8. Installation of the bottom mounting on the base plate.

The next component is the box barrel, as depicted in Figure 9. The internal dimensions of the box barrel are 300 mm (length) × 300 mm (width) × 150 mm (height). To prevent failure under high pressure, the thickness of the box barrel and the stiffeners was increased to 13 mm. The viscous fluid contained within the box barrel plays a crucial role in dissipating vibration energy.

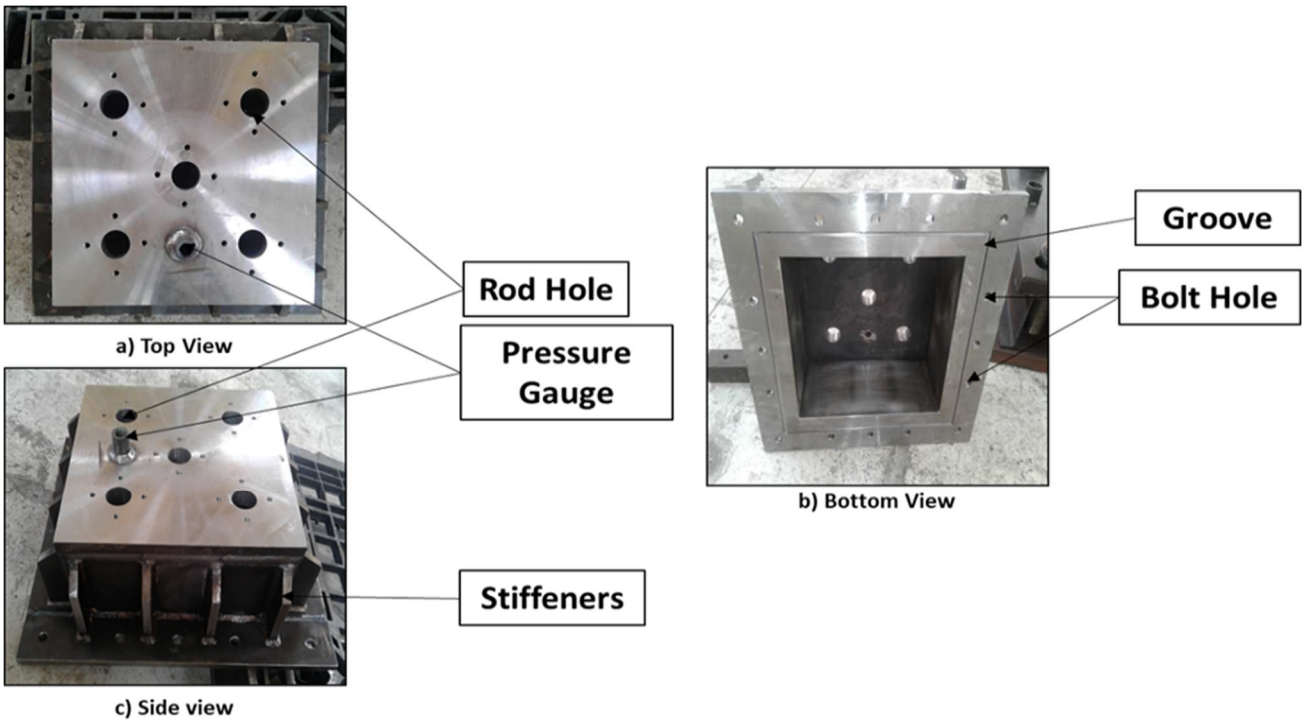

Figure 9. Box barrel.

The top of the box barrel features five holes. Figure 10 illustrates that four piston rods are positioned at the edges of each hole, allowing the rods to move within them. The central hole is designated for filling the viscous fluid. The piston rods connect the piston plate inside the barrel to the head mounting, as shown in Figure 11.

Figure 10. Piston rod.

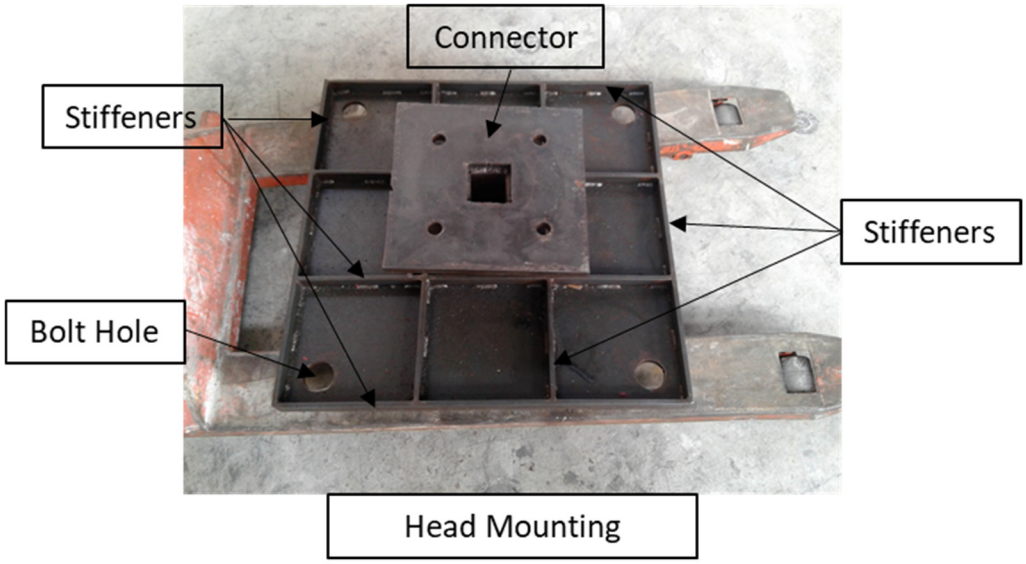

Figure 11. Head mounting.

A piston plate was installed inside the box barrel, as shown in Figure 12. Each piston plate has dimensions of 298 mm (length) × 298 mm (width) × 20 mm (thickness), with orifice diameters of 10 mm, 5 mm, 2 mm, and 1 mm.

Figure 12. Piston plate.

The configuration of the piston plate was determined based on the placement of open orifices. Figure 13 illustrates the positions of open orifices on the piston plate, marked with a green "X" and closed orifices marked with a red circle. During the experimental testing, various diameters and configurations of these orifices were installed inside the box barrel, and tests were conducted under cyclic loads.

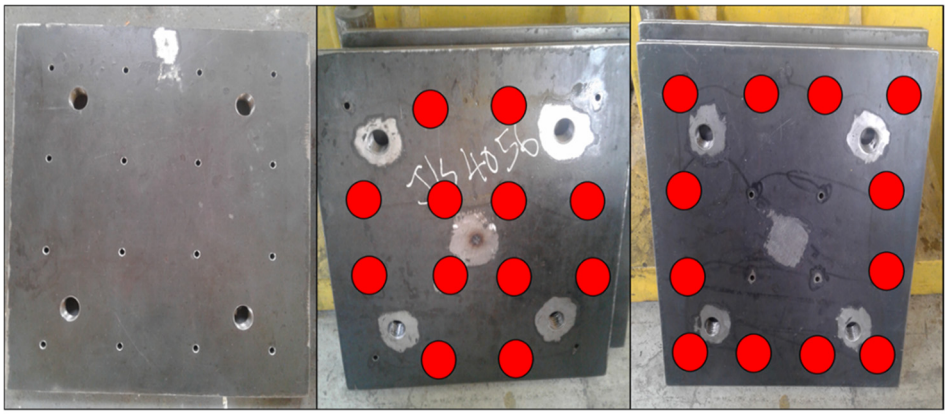

Figure 13. Configuration of orifices on the piston plate.

In the next step, the piston plate and piston rod were fixed inside the box barrel. Subsequently, the box barrel was secured onto the bottom mounting, which was already fixed to the base plate. Figure 14 shows the four piston rods secured to the piston plate (a). Following this, the components were installed inside the box barrel (b). Figure 15 depicts the box barrel positioned on top of the bottom mounting and fastened with bolts and nuts. High-strength bolts and nuts were used to ensure a secure attachment of the bottom mounting to the box barrel.

Figure 14. Fixing the piston plate into the box barrel.

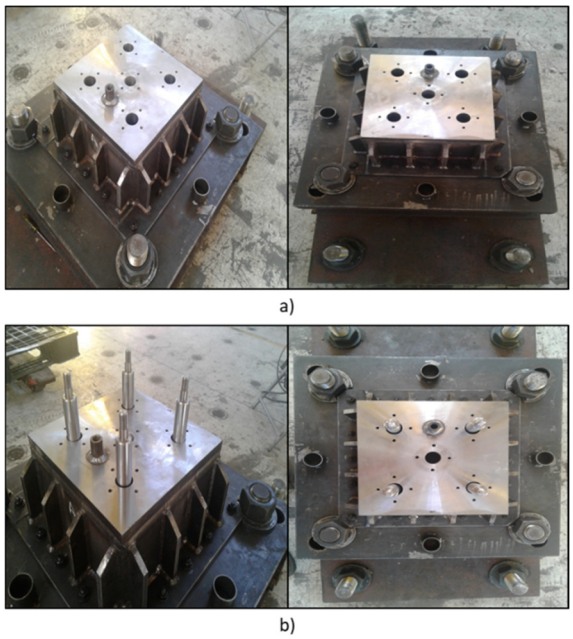

Figure 15. Installation of the box barrel on the bottom mounting; (**a**) without piston rod, (**b**) with piston rod.

Every hole on top of the box barrel was closed using capping, as shown in Figure 16. Capping is a crucial component that ensures the viscous fluid inside the box barrel remains contained during piston rod movement. It also acts as a seal to prevent pressure from escaping the box barrel. Figure 17 shows two types of capping: (a) includes both an oil seal and an oil ring and (b) uses only an oil seal. The oil ring and oil seal are designed to withstand high pressure and temperature, effectively preventing leakage and maintaining pressure inside the barrel.

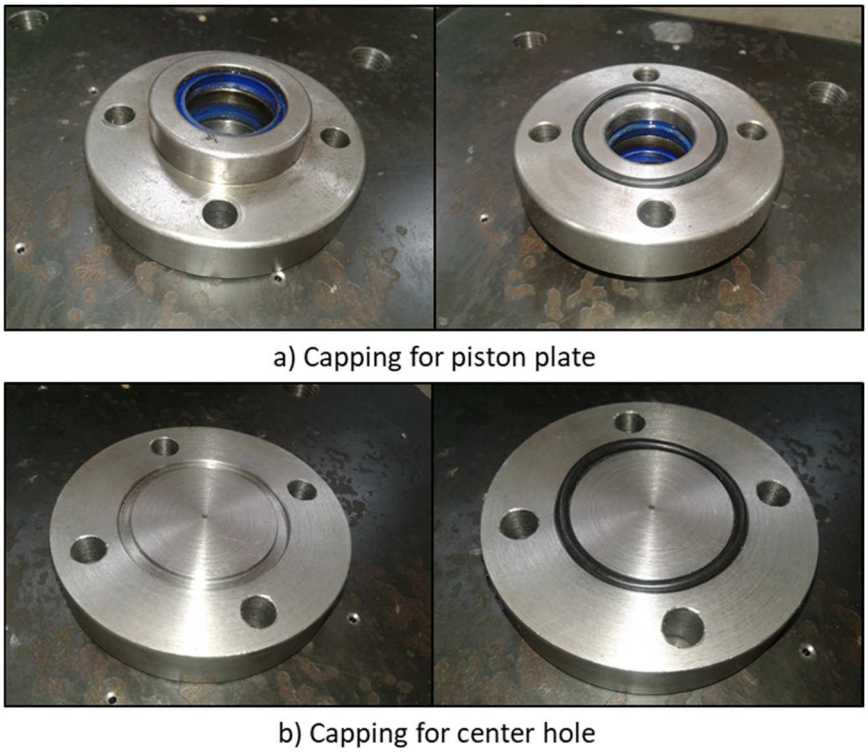

Figure 16. (**a**) Capping for piston plate; (**b**) capping for centre hole.

Figure 17. Installation of capping on top of the box barrel.

Figure 17 shows the installation of the capping on top of the box barrel. The capping is secured with high-strength bolts. At this stage, the viscous fluid was filled into the barrel. The oil ring and oil seal were employed to prevent leakage at the joint or connection points. Figure 18 illustrates the connection between the box barrel and the bottom mounting, highlighting the use of an oil ring in the groove to ensure a tight seal.

Figure 18. Details of oil ring.

Figure 18 presents the details and location of the oil ring used. The oil ring is positioned in the groove to prevent the viscous fluid from leaking between the two plates. It is also used in the groove of the box barrel. In this study, it is assumed that the fluid transfers to the other side of the barrel solely through the orifices during the movement of the piston plate.

Figure 19 shows the viscous plane damper with the piston installed and ready for testing.

Figure 19. Installation of head mounting on top of viscous damper.

4. Experimental Setup

The performance of the developed viscous plane damper was evaluated through experimental testing conducted at the Structural Laboratory, Department of Civil Engineering, University Putra. The purpose of the test was to assess the damper's efficiency and collect relevant data. The testing results were analyzed to determine the effectiveness of the new viscous plane damper in dissipating vibration energy. Figure 20 illustrates the experimental setup used for testing the viscous plane damper. In this study, the selected parameters include piston velocity, plate movement configuration, and the diameter of the orifice. Table 3 summarizes the parameters evaluated during the experimental testing and numerical model analysis to determine the device's performance and functionality.

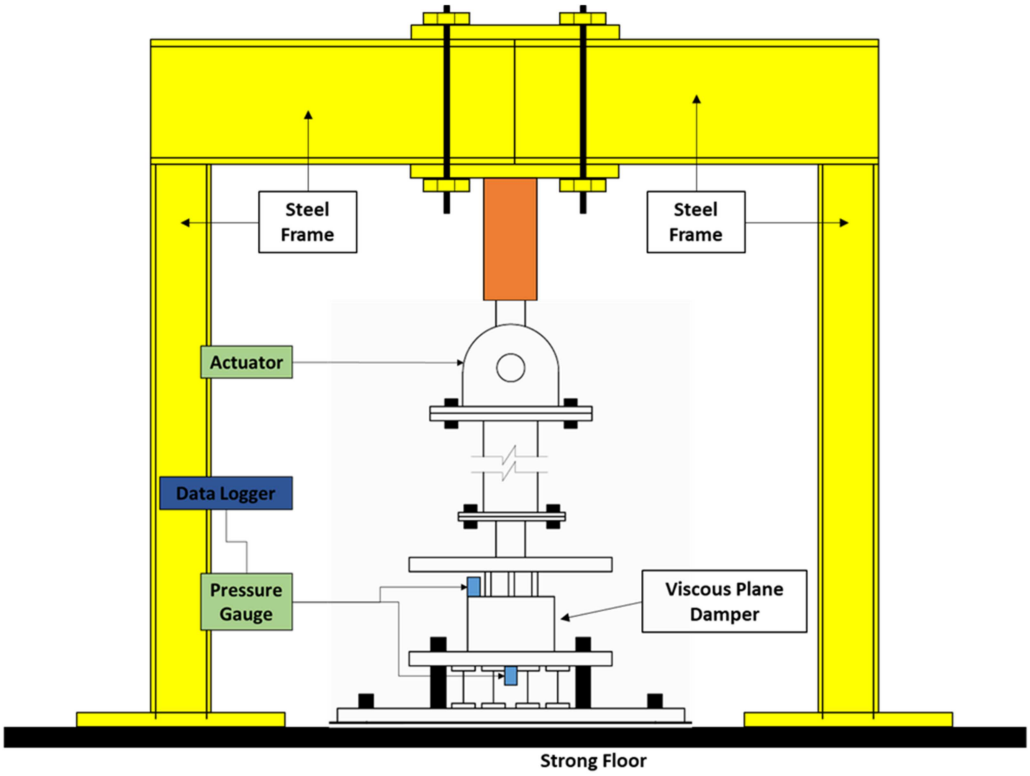

Figure 20. Experimental setup.

Table 3. Study parameters.

Dimension of Viscous Plane Damper (mm)	Thickness of Piston Plate (mm)	Movement of Piston Plate (mm)	Configuration A (Case A)	Configuration B (Case B)	Configuration C (Case C)
			Diameter (mm)		
300 × 300 × 150	20	10 20 30 40	1, 2, 5, 10		

The materials used in the development of the new viscous plane damper included standard steel for the structural components and a viscous fluid contained within the box barrel.

The viscous plane damper was set up vertically on the strong floor, with a dynamic actuator mounted on a robust support frame and connected to the head mounting using extension bolts and nuts, as shown in Figure 21. The damper's dimensions were 0.3 m × 0.3 m × 0.15 m, with a height of 0.15 m, and the piston plate inside the box barrel was capable of ±60 mm movement. To measure the pressure within the box barrel, two pressure gauges were installed at the top and bottom of the damper, connected to a data logger. Figure 21 illustrates the actual setup used for testing in the structural laboratory.

Figure 21. Setup of testing for viscous plane damper and dynamic actuator.

Cyclic Loading

The cyclic load was applied to the piston using a dynamic actuator with a load capacity of 300 kN. Table 4 details the velocities of the piston plate used during the experimental testing. The piston plate was subjected to movements with velocities ranging from 10 mm to 40 mm, and the corresponding damping forces were recorded. Although the allocated space allowed piston plate movement up to ±65 mm, the plate did not exceed the recorded movement values. Additional space was provided to accommodate any unpredictable movements during testing. Various movements and velocities were applied for each test, considering different configurations and orifice diameters.

Table 4. Velocity of piston plate.

Movement of Piston Plate (mm)	Configuration A					Configuration B					Configuration C				
	Velocity (mm/s)														
	1	**2**	**5**	**8**	**10**	**1**	**2**	**5**	**8**	**10**	**1**	**2**	**5**	**8**	**10**
10	--	--	5.7	--	5.7	6.2	6.2	--	--	--	6.2	6.2	--	--	--
20	--	--	13.7	--	14.2	13.8	13.9	--	--	--	13.9	13.9	--	--	--
30	--	--	16.7	--	17.5	16.1	17.1	--	--	--	16.7	16.7	--	--	--
40	--	--	17.7	--	18.4	17.7	17.8	--	--	--	0.0	17.7	--	--	--

Figure 22 shows displacement versus time for cyclic loading during the testing. The graph illustrates how the load was applied to evaluate the performance of the viscous plane damper and ensure it operated smoothly. The piston plate movement was recorded over a range of 10 mm to 40 mm across various time intervals.

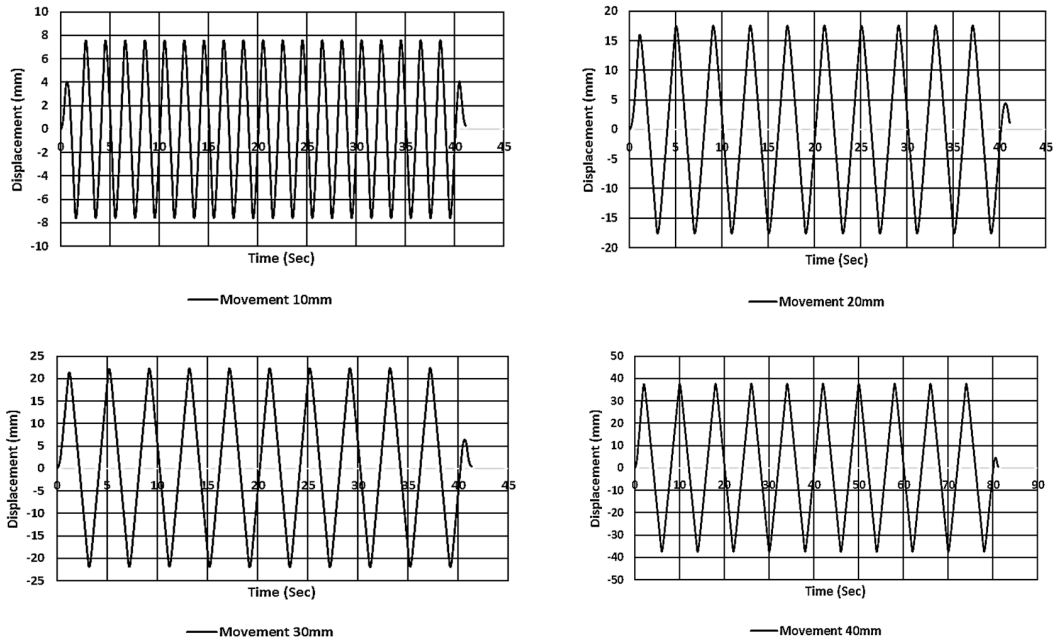

Figure 22. Piston plate movement for each experimental test.

5. Results of Experimental Test

The objective of the experimental testing was to assess the performance of the newly designed viscous plane damper. The experimental setup aimed to simulate the actual installation of the damper on structures. Data collected from the tests were analyzed and organized into three cases: Configurations A, B, and C. Testing involved varying orifice diameters and piston plate movements ranging from 10 mm to 40 mm.

5.1. Configuration A

Configuration A featured 16 orifices evenly distributed on the piston plate. Table 5 presents the damping force generated by the viscous plane damper for Configuration A with 10 mm and 5 mm diameter orifices. The results indicate that the damper's performance, in terms of damping force, was very low. Consequently, tests for the 5 mm and 10 mm diameters were not conducted further. This limited capacity is attributed to the large total cross-sectional open area, allowing the viscous fluid to flow too easily through the orifices, thereby reducing the pressure inside the box barrel.

Table 5. Damping force produced for Configuration A.

Experimental Results for Configuration A		
Movement of Piston Plate (mm)	Diameter (mm)	
	10	5
	Force (kN)	
10	1.14	0.58
20	2.54	8.56
30	2.69	8.37
40	2.83	9.17

For Configuration A, the damping force with 5 mm diameter orifices was three times higher than with 10 mm diameter orifices when the plate movement ranged between 20 mm and 40 mm. However, the damping force for the 10 mm diameter orifices was inadequate for effective vibration energy dissipation. As a result, the experimental testing continued with Configurations B and C, which used only 2 mm and 1 mm diameter orifices.

5.2. Configuration B

Configuration B featured four orifices located at the edges of the piston plate. Cyclic load testing was conducted for Configuration B with orifices of 1 mm and 2 mm diameters, and piston plate movements ranged from 10 mm to 40 mm.

Figures 23 and 24 illustrate the time history and hysteresis results for Configuration B. The results show that the load generated by the viscous plane damper increases with both displacement and velocity. As the movement velocity of the piston plate increases, the load produced inside the box barrel also increases. This increase in load is attributed to the fluid movement within the box barrel. Notably, the total cross-sectional open area does not significantly affect the fluid flow through the orifices when it comes to increasing the load produced in the barrel. However, a fixed cross-sectional open area does contribute to an increase in the damping force.

The peak values of the damping force for different cyclic test amplitudes are listed in Table 6. The results indicate that the damping force increased with the piston plate movement. For Configuration B, the force generated by the viscous plane damper was higher compared to that for Configuration A. This observation aligns with the findings reported by Alessandro Palmeri (2006), which demonstrated that the capacity of a damper to dissipate external energy is influenced by the velocity of the viscous fluid moving inside the damper. When the orifice diameter is larger, the velocity of the fluid tends to decrease due to the lower pressure required to push the fluid through [33]. Similarly, Hiroshi Yamaguchi, Xin-Rong Zhang, Xiao-Dong Niu, and K. Nishioka (2010) tested electro-rheological fluid dampers with a constant orifice diameter [34].

The results Indicate that varying fluid viscosity can enhance the force exerted by the damper to reduce piston plate movement. Table 6 shows the force capacity of the viscous plane damper for Configuration B, where the performance notably improved, especially with the 1 mm diameter orifice, which was 50% higher than that of the 2 mm diameter orifice. The same type of fluid was used across tests to ensure consistency in the results.

Reducing the cross-sectional area of the orifices increased the fluid pressure, thus generating higher drop pressure inside the box barrel, which, in turn, led to a greater damping force. This observation aligns with the experimental study by Chien-Yuan Hou (2008), which demonstrated that increased liquid compression within the barrel could generate more force. On average, the load produced by Configuration B with the 1 mm diameter orifice was 90% higher than that with the 2 mm diameter orifice across piston plate movements ranging from 10 mm to 40 mm [35].

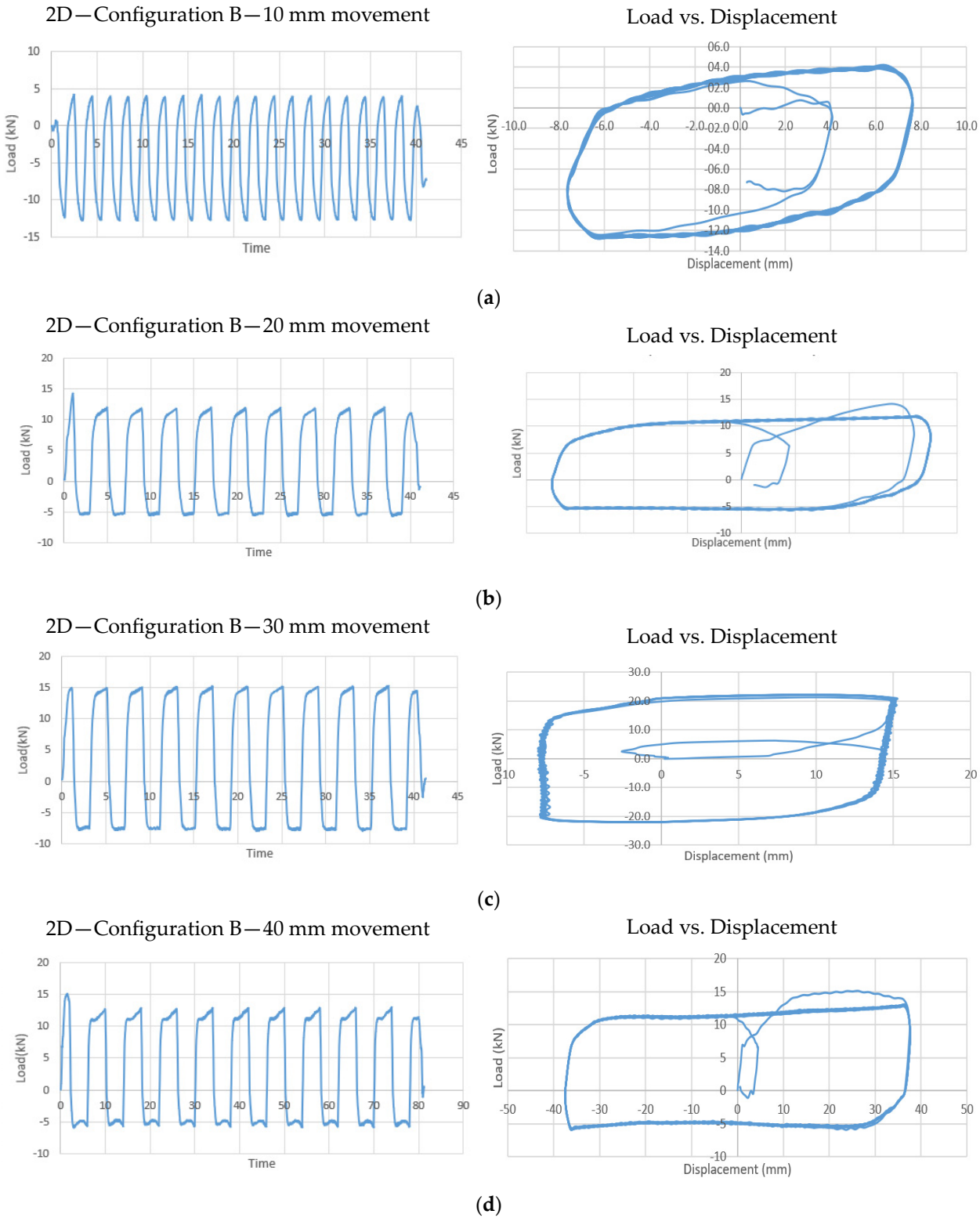

Figure 23. Cyclic load for 2 mm diameter for Configuration B. (**a**) Load generated by 10 mm movement; (**b**) load generated by 20 mm movement; (**c**) load generated by 30 mm movement; (**d**) load generated by 40 mm movement.

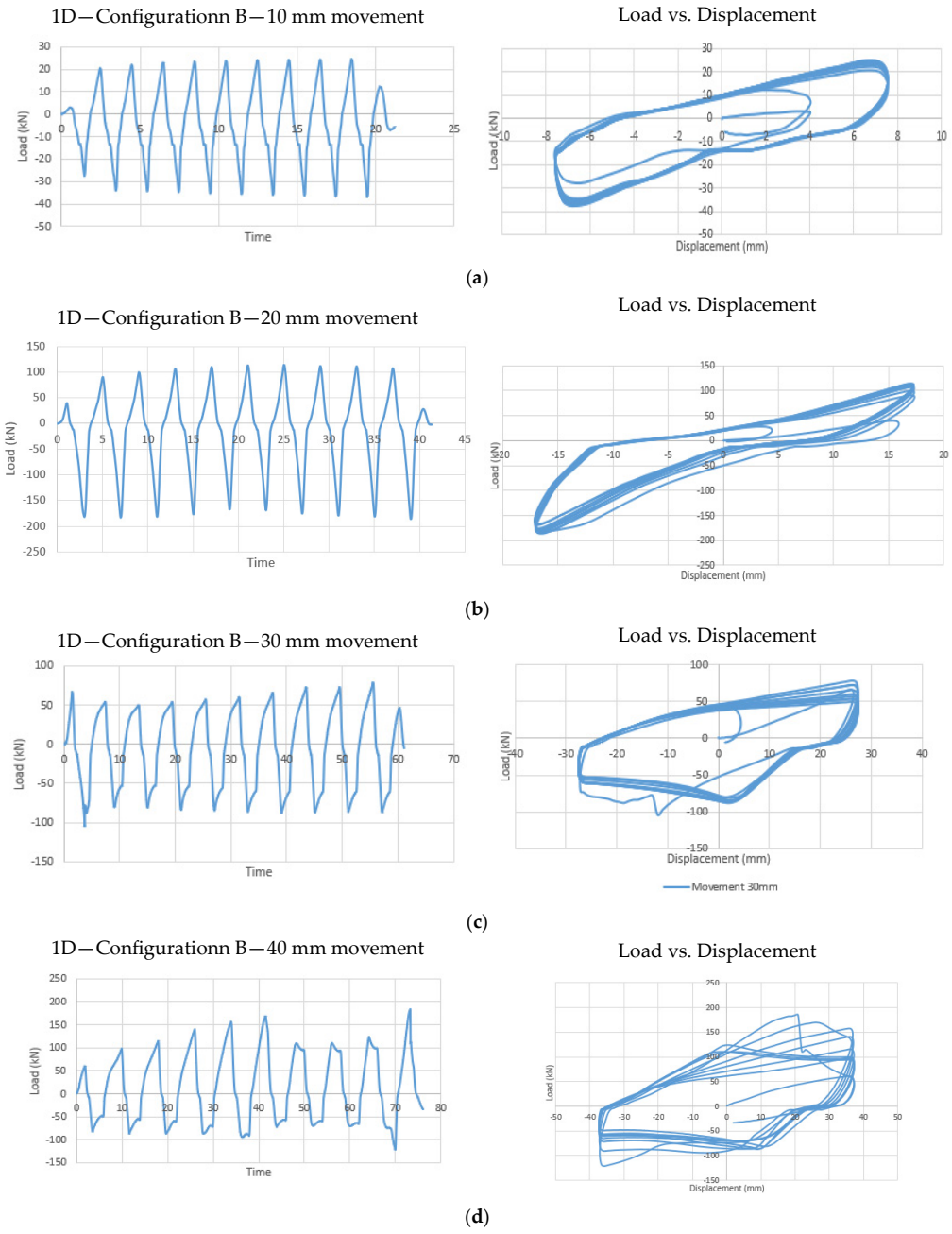

Figure 24. Cyclic load for 1 mm diameter for configuration B. (**a**) Load generated by 10 mm movement; (**b**) load generated by 20 mm movement; (**c**) load generated by 30 mm movement; (**d**) load generated by 40 mm movement.

Table 6. Load produced for Configuration B.

Movement of Piston Plate (mm)	Diameter (mm)		Difference (%)
	2	1	
	Force (kN)		
10	21.96	24.56	11.84
20	37.57	100.73	168.11
30	79.82	127.83	60.15
40	71.12	184.00	158.72

5.3. Configuration C

Four holes were drilled into the 20 mm thick piston plate, with orifices located at the center of the plate, spaced evenly. Despite having the same total cross-sectional open area as Configuration B, Configuration C demonstrated different performance results.

Figures 25 and 26 display the results of cyclic load testing and the load–displacement graphs for Configuration C. The figures reveal a similar pattern to the results for Configuration B. However, despite having the same total cross-sectional open area, Configuration C produced a higher load than Configuration B. This improvement is attributed to the placement of orifices at the center of the piston plate, which led to a more uniform distribution of viscous fluid flow compared to Configuration B.

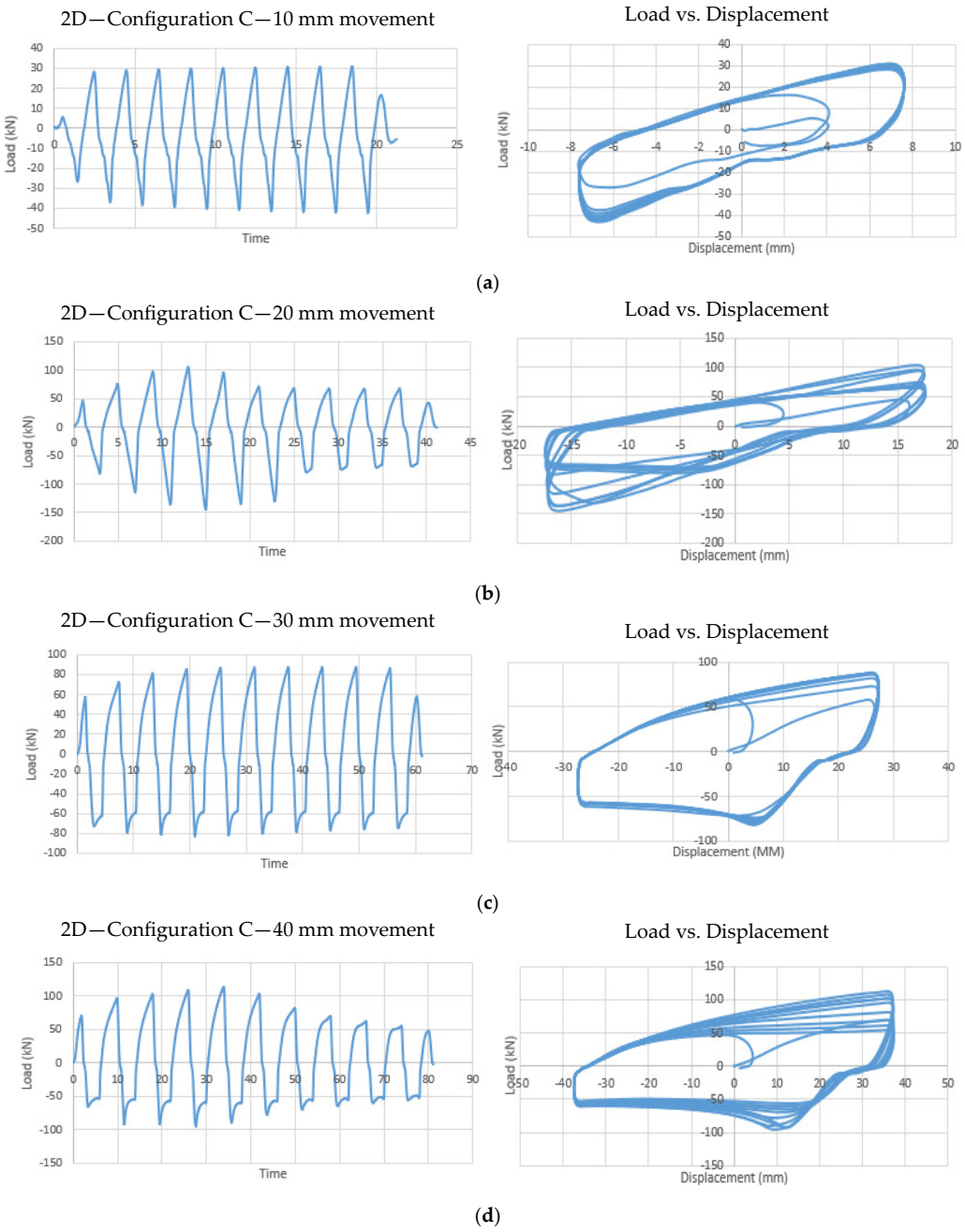

Figure 25. Cyclic load for 2 mm diameter for Configuration C. (**a**) Load generated by 10 mm movement; (**b**) load generated by 20 mm movement; (**c**) load generated by 30 mm movement; (**d**) load generated by 40 mm movement.

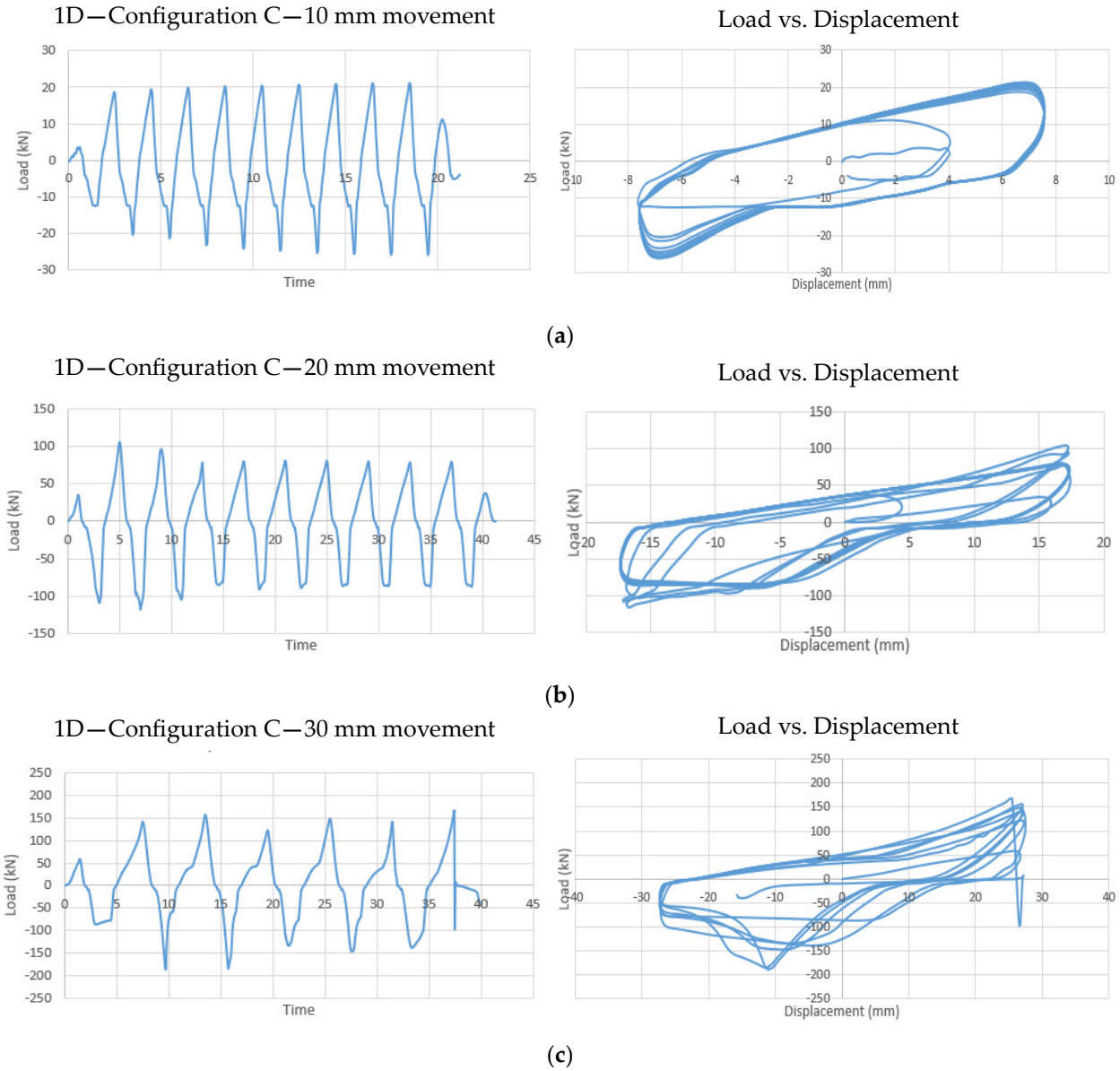

Figure 26. Cyclic load for 1 mm diameter for Configuration C. (**a**) Load generated by 10 mm movement; (**b**) load generated by 20 mm movement; (**c**) load generated by 30 mm movement.

Table 7 shows the damping force capacity of the viscous plane damper for Configuration C. The performance improved notably, especially with the 1 mm diameter orifices. The smaller size of these orifices enhanced fluid flow control through the holes, increasing the drop pressure and thereby boosting the damping force. This finding aligns with the study by Ehsan Kabiri Rahani et al. (2009), which demonstrated that smaller orifices lead to higher drop pressures, resulting in greater damping force inside the barrel and better reduction of building movement against external forces such as seismic activity and typhoons [36].

The load produced by Configuration C with 1 mm diameter orifices was significantly higher than that of the 2 mm diameter orifices. On average, the load with 1 mm orifices was over 40% greater than with 2 mm orifices. This increase in load is attributed to the improved fluid flow dynamics within the box barrel due to piston plate movement, highlighting the importance of orifice size in affecting the damper's performance.

Table 7. Load produced on Configuration C.

Movement of Piston Plate (mm)	Diameter (mm)		Difference (%)
	2	1	
	Force (kN)		
10	21.05	30.47	44.75
20	87.69	104.83	19.55
30	104.50	166.53	59.36
40	112.92		

5.4. Combination of Configuration B and C

Figure 27 shows the damping ratio for each diameter of orifices and configuration, calculated from the hysteresis graphs obtained during experimental testing.

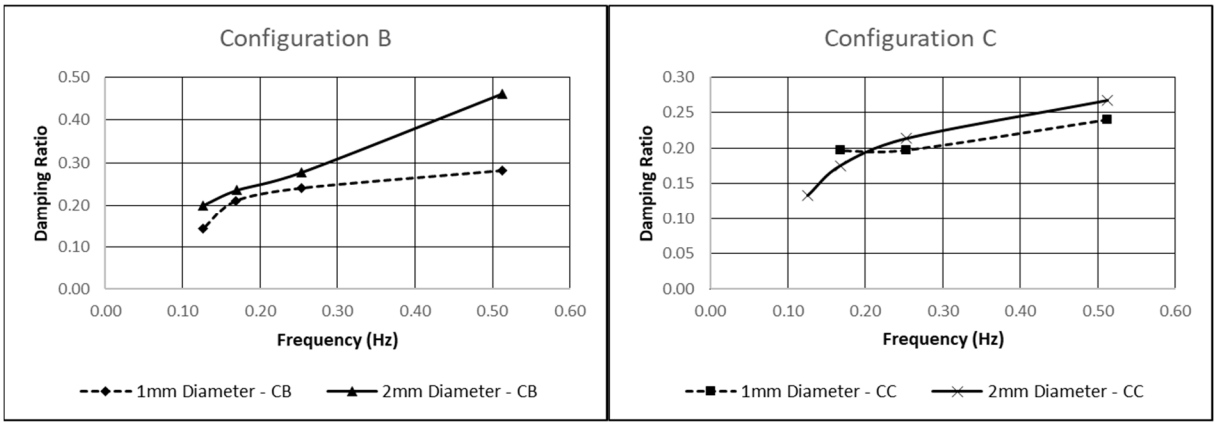

(**a**) (**b**)

Figure 27. (**a**) Damping ratio for Configuration B, (**b**) damping ration for Configuration C.

Configurations B and C, which feature four orifices located at the edge and center of the piston plate, respectively, display different damping ratios. As illustrated in Figure 27, the damping ratio for the damper with a 2 mm orifice diameter is higher than for the 1 mm orifice diameter. Although the damper with the 1 mm diameter orifices generates higher force due to the increased resistance to fluid flow, the position of the orifices significantly influences the damping ratio.

In particular, the configuration with orifices at the edges of the piston plate (Configuration B) shows a higher damping coefficient and energy dissipation compared to Configuration C, where the orifices are positioned at the center of the piston plate. This indicates that the placement of orifices around the edges enhances the overall performance of the viscous plane damper.

6. Comparison of the Developed Viscous Plane Damper with Other Damper Devices

In this section, an attempt has been made to compare the performance of the developed viscous plane damper with some of the conventional vibration-damping devices that are reported in the literature. Therefore, a few different types of damper devices, including viscous dampers [37,38], fluid viscous dampers [22,39], rubber bracing damper systems [23], and Volumetric Compression Restrainers [40] were considered, and their performance was compared in terms of damping force and effective damping stiffness. Also, the required space for the installation of various damping devices was compared to highlight the advantage of the proposed viscous plane damper device for implementation in very limited space.

The comparison results are presented in Table 8 and indicate that the newly developed viscous plane damper demonstrates significant advantages in both space efficiency and performance when compared to other damping systems. Traditional dampers, such as fluid viscous dampers and rubber bracing damper systems, require substantially more installation space. For example, the fluid viscous damper [24] occupies a space of 1.90 m^2, and the rubber bracing damper system [34] needs as much as 5.12 m^2. In contrast, the viscous plane damper requires only 0.045 m^2 of space—over 97% smaller than the fluid viscous damper and 99% smaller than the rubber bracing damper system. This makes the viscous plane damper particularly well-suited for installation in confined spaces, such as structural gaps or joints, where larger devices are impractical.

Table 8. Comparison of the developed viscous plane damper with other damper devices.

Damping Type		Viscous Plane Damper (Present Study)	Fluid Viscous Damper [22]	Fluid Viscous Damper [39]	Rubber Bracing Damper System [23]	Volumetric Compression Restrainer [40]	Viscous Damper [37]	Viscous Damper System [38]
Dimension	Length (m)	0.15	0.97	1	1.6	1.6	0.49	0.59
	Diameter/Width (m)	0.3 × 0.3	0.175	0.5	0.27	0.27	0.14	0.05
Required Space (Height × Width) (m)		0.15 × 0.3	1.95 × 0.97	1.5 × 1	3.2 × 1.6	3.2 × 1.6	0.98 × 0.49	1.19 × 0.59
Required Space Area (m^2)		0.045	1.9	1.5	5.12	5.12	0.48	0.7
Comparison of Area (%)		41.2	112	32.23	112	112	9.67	14.5
Damping Force (KN)		184	300	13.1	247	320	300	8
Effective Damping (N.s/mm)		4090	2203	5100	1244	1000	1650	100,000
Effective Stiffness (N/mm)		5000	3333	0	2400	1200	3750	0
Comparison with Present Study	Damping Force (%)	—	63	34	74	63	92	96
	Effective Damping (%)	—	46	69	75	60	24	23
	Effective Stiffness (%)	—	33	52	76	25	100	100

When it comes to performance, the viscous plane damper's compact size does not compromise its effectiveness. It produces a damping force of 184 kN, which is 63% of the force generated by a conventional fluid viscous damper (300 kN). Although slightly lower, this is still a highly efficient output, considering its much smaller size. Additionally, the viscous plane damper has an effective damping capacity of 4090 N.s/mm, which is 85% higher than the fluid viscous damper's effective damping of 2203 N.s/mm, demonstrating its ability to dissipate significant amounts of energy despite its reduced size. The effective stiffness of the viscous plane damper is 5000 N/mm, representing a 50% increase over the fluid viscous damper's stiffness of 3333 N/mm.

In summary, the viscous plane damper offers exceptional space-saving benefits with a 96–99% reduction in required space compared to traditional dampers while still delivering comparable and, in some cases, superior performance in terms of damping force and energy dissipation. These attributes make it an ideal choice for structures with space constraints without sacrificing structural protection and vibration control.

This device is specifically designed for gaps within structures that have limited space, where it is impractical to use conventional viscous dampers as diagonal members or bracing systems. These include gaps between two structures, joints in adjacent buildings, or within jetty platforms. The design has been optimized through experimental testing on a prototype of the viscous plane damper using various orifice numbers and diameters to achieve optimal performance.

Since the device relies on viscous material for energy dissipation, its functionality and the generated damping force are velocity-dependent. Therefore, the device's performance is influenced by movement velocity, and at low velocities, its effectiveness may be reduced.

In order to comprehensively assess the device's performance, it is proposed that future research will test the developed plane damper device under wind loads and realistic seismic excitation. Also, developing a constative model for the proposed damper device makes the possibility of using the finite element method to simulate the function of the viscous plane damper.

The primary advantage of the newly developed viscous plane dampers, compared to conventional cylindrical viscous dampers, is their ability to be installed in very limited spaces, such as within gaps and joints of structures. Unlike conventional viscous dampers, which require longitudinal space within a structure, the viscous plane damper is designed to fit within limited spaces. This is particularly useful in structures like jetties, offshore platforms, or retrofitted buildings where space is constrained. The viscous plane damper's square-shaped design allows it to be installed in areas where traditional dampers are impractical.

The MTS dynamic actuator (USA) with a force capacity of 1000 KN has been implemented to conduct this test. In the initial attempt, there was some leaking during the test; through applying some improvement in the sealing of parts and overall design of the device, there was no further leaking in the subsequent tests.

The experimental test results indicate that the proposed viscous plane damper device can generate 184 KN damping force in 0.25 Hz load frequency. This device functions using viscous material; therefore, the performance of the device is dependent on the load frequency. As can be seen in the results, the generated damping force in low frequencies is considerably low.

7. Conclusions

In this study, a new viscous plane damper (VPD) was developed to address the challenges of installing conventional viscous dampers in limited spaces. The new design of the viscous plane damper was evaluated to determine its capability for installation in confined spaces. Despite having the same damping force capacity, the new damper is lighter and shorter but wider compared to typical viscous dampers. It is modular designed, which allows for on-site assembly, making it more practical for installation in tight spaces compared to conventional dampers that are pre-manufactured.

The experimental test results indicate that the developed viscous plane damper (VPD) demonstrates high performance in energy dissipation and vibration control, particularly in confined spaces. A series of tests were conducted, varying the number and diameter of orifices on the piston plate, to assess the damper's performance. Three different configurations with 1 mm, 2 mm, 5 mm, and 10 mm diameter orifices were tested under cyclic loading with piston plate displacements ranging from 10 mm to 40 mm using a dynamic actuator.

The results show that smaller orifices (1 mm and 2 mm) generated significantly higher damping forces compared to larger ones. For instance, the configuration with 1 mm orifices produced a damping force 90% higher than that with 2 mm orifices. The damper achieved a maximum damping force of 184 kN with an effective damping capacity of 4090 N.s/mm, which represents an 85% increase in performance compared to conventional systems. Additionally, the VPD exhibited 5000 N/mm effective stiffness, improving the structural stability under dynamic loads. These findings confirm that the optimal orifice configuration and diameter significantly enhance the VPD's ability to dissipate energy, making it an ideal solution for space-constrained structural applications.

Author Contributions: Conceptualization, M.R.B.M.A. and F.H.; Methodology, M.R.B.M.A. and F.H.; Software, M.R.B.M.A.; Formal analysis, M.R.B.M.A.; Investigation, M.R.B.M.A.; Resources, F.H.; Data curation, M.R.B.M.A.; Writing—original draft, M.R.B.M.A.; Writing—review and editing, F.H.; Visualization, M.R.B.M.A.; Supervision, F.H.; Project administration, F.H.; Funding acquisition, F.H. All authors have read and agreed to the published version of the manuscript.

Funding: This research received financial support from the University Putra Malaysia (UPM) under the Putra Grant Research Project, No. 9531200.

Institutional Review Board Statement: Not applicable.

Informed Consent Statement: Not applicable.

Data Availability Statement: All data generated or analyzed during this study are included in this published article.

Conflicts of Interest: The authors declare no conflicts of interest.

References

1. Zheng, W.; Wang, H.; Tan, P.; Li, J.; Liu, Y. Numerical Modeling and Experimental Validation of Sliding LRBs Considering Physical Strength Degradation. *Eng. Struct.* **2022**, *262*, 114374. [CrossRef]
2. Zheng, W.; Tan, P.; Li, J.; Wang, H.; Liu, Y.; Yang, K. Seismic Performance Upgrading of Bridges Using Superelastic Pendulum Isolators with Variable Stiffness Considering Temperature Effects. *Eng. Struct.* **2023**, *275*, 115244. [CrossRef]
3. Wang, S.; Yuan, Y.; Tan, P.; Li, Y.; Zheng, W.; Zhang, D. Experimental Study and Numerical Model of a New Passive Adaptive Isolation Bearing. *Eng. Struct.* **2024**, *308*, 118044. [CrossRef]
4. Kareem, A.; Kijewski, T.; Tamura, Y. Mitigation of motions of tall buildings with specific examples of recent applications. In *Wind and Structures*, 2nd ed.; Kim, C.-H., Ed.; Techno-Press: Jeju, Republic of Korea, 1999; Volume 2, pp. 201–251. [CrossRef]
5. Hejazi, F.; Noorzaei, J.; Jaafar, M.S. Application of nonlinear damper in reinforced concrete structure control. In *Challenges, Opportunities and Solutions in Structural Engineering and Construction*; Smith, A.B., Ed.; Elsevier: Amsterdam, The Netherlands, 2010; pp. 25–30.
6. Petti, L.; De Iuliis, M. Torsional seismic response control of asymmetric-plan systems by using viscous dampers. *Eng. Struct.* **2008**, *30*, 3377–3388. [CrossRef]
7. Hejazi, F.; Jilani, S.; Noorzaei, J.; Chieng, C.Y.; Jaafar, M.S.; Abang Ali, A.A. Effect of Soft Story on Structural Response of High Rise Buildings. *Mater. Sci. Eng.* **2011**, *17*, 012034. [CrossRef]
8. Rouhani, B.; Aghayari, R.; Mousavi, S.A. Fluid Viscous Dampers in Tackle-Damper Configuration: An Experimental Study. *Eng. Struct.* **2024**, *321*, 118927. [CrossRef]
9. Zoccolini, L.; Bruschi, E.; Cattaneo, S.; Quaglini, V. Current Trends in Fluid Viscous Dampers with Semi-Active and Adaptive Behavior. *Appl. Sci.* **2023**, *13*, 10358. [CrossRef]
10. Zhou, Y.; Sebaq, M.S.; Xiao, Y. Energy dissipation demand and distribution for multi-story buildings with fluid viscous dampers. *Eng. Struct.* **2022**, *253*, 113813. [CrossRef]
11. Zhou, Y.; Lu, X.; Weng, D.; Zhang, R. A practical design method for reinforced concrete structures with viscous dampers. *Eng. Struct.* **2012**, *39*, 187–198. [CrossRef]
12. Cucuzza, R.; Domaneschi, M.; Greco, R.; Marano, G.C. Numerical models comparison for fluid-viscous dampers: Performance investigations through Genetic Algorithm. *Comput. Struct.* **2023**, *288*, 107122. [CrossRef]
13. Shang, F.; Liu, W.; Zhang, Q.; Xu, H.; Guo, Y. Shaking table test and seismic behaviour evaluation of viscous damping wall with amplification mechanism. *Eng. Struct.* **2023**, *284*, 115974. [CrossRef]
14. Tang, L.; Li, J.; Xie, Y.; Tian, Z. Experimental Research on Dynamic Performance of Viscous Fluid Damper. In Proceedings of the 2021 4th International Symposium on Traffic Transportation and Civil Architecture (ISTTCA), Suzhou, China, 12–14 November 2021; IEEE: New York, NY, USA, 2021; p. 437, ISBN 978-1-6654-2592-6.
15. Faruk, M.O.; Singh, S.K.; Mondal, S. Comparative study of buckling restrained braces and fluid viscous damper applied in an RCC structure following pushover analysis. *Mater. Today Proc.* **2023**. [CrossRef]
16. Parajuli, S.; Pokhrel, P.; Suwal, R. A comprehensive study of viscous damper configurations and vertical damping coefficient distributions for enhanced performance in reinforced concrete structures. *Asian J. Civ. Eng.* **2024**, *25*, 1043–1059. [CrossRef]
17. Lan, X.; Wei, G.; Zhang, X. Study on the Influence and Optimization Design of Viscous Damper Parameters on the Damping Efficiency of Frame Shear Wall Structure. *Buildings* **2024**, *14*, 497. [CrossRef]
18. Lan, X.; Zhang, L.; Sun, B.; Pan, W. Study on the Damping Efficiency of a Structure with Additional Viscous Dampers Based on the Shaking Table Test. *Buildings* **2024**, *14*, 1506. [CrossRef]
19. Yang, C.; Wang, H.; Xie, L.; Li, A.; Wang, X. Experimental and Theoretical Investigations on an Asynchronized Parallel Double-Stage Viscous Fluid Damper. *Struct. Control Health Monit.* **2024**, *2024*, 14. [CrossRef]
20. He, W.; Xu, H.; Xu, Z.; Liu, W. Experimental investigation and earthquake response analysis of a multilayer viscous damping wall with amplified deformation. *Eng. Struct.* **2022**, *251*, 113427. [CrossRef]
21. Hu, S.; Koetaka, Y.; Chen, Z.-P.; Zhu, S.; Alam, M.S. Hybrid Self-Centering Braces with NiTi-SMA U-Shaped and Frequency-Dependent Viscoelastic Dampers for Structural and Nonstructural Damage Control. *Eng. Struct.* **2024**, *308*, 117920. [CrossRef]
22. Farahpour, H.; Hejazi, F. Development of integrated semi-active adaptive vibration control system for bridges subjected to traffic loads. *Structures* **2023**, *51*, 1773–1794. [CrossRef]
23. Hejazi, F.; Farahpour, H.; Ayyash, N. Seismic performance of structure equipped with a new rubber bracing damper system. *Arch. Civ. Mech. Eng.* **2024**, *24*, 46. [CrossRef]

24. Hejazi, F.; Noorzaei, J.; Jaafar, M.S.; Abang Abdullah, A.A. Earthquake Analysis of Reinforce Concrete Framed Structures with Added Viscous Dampers. *Int. J. Appl. Sci. Eng. Technol.* **2009**, *3*, 205–210.
25. Love, J.S.; Tait, M.J. A preliminary design method for tuned liquid dampers conforming to space restrictions. *Eng. Struct.* **2012**, *40*, 187–197. [CrossRef]
26. Love, J.S.; Tait, M.J. Multiple Tuned Liquid Dampers for Efficient and Robust Structural Control. *J. Struct. Eng.* **2015**, *6*, 1–6. [CrossRef]
27. Silwal, B.; Micheal, R.J.; Ozbulut, O.E. A superelastic viscous damper for enhanced seismic performance of steel moment frames. *Eng. Struct.* **2015**, *105*, 152–164. [CrossRef]
28. Su, H.; Zhu, L.; Meng, L. The Shaking Table Test and the Numerical Analysis on a Novel Viscous Damper Installation Configuration. *J. Build. Eng.* **2024**, *83*, 108418. [CrossRef]
29. Curadelli, R.O.; Riera, J.D. Reliability based assessment of the effectiveness of metallic dampers in buildings under seismic excitations. *Eng. Struct.* **2004**, *26*, 1931–1938. [CrossRef]
30. Ras, A.; Boumechra, N. Seismic energy dissipation study of linear fluid viscous dampers in steel structure design. *Alex. Eng. J.* **2016**, *55*, 2821–2832. [CrossRef]
31. Martinez-Rodrigo, M.; Romero, M.L. An optimum retrofit strategy for moment resisting frames with nonlinear viscous dampers for seismic applications. *Eng. Struct.* **2003**, *25*, 913–925. [CrossRef]
32. Jin, Q.; Li, X.; Sun, N.; Zhou, J.; Guan, J. Experimental and numerical study on tuned liquid dampers for controlling earthquake response of jacket offshore platform. *Mar. Struct.* **2007**, *20*, 238–254. [CrossRef]
33. Palmeri, A. Correlation coefficients for structures with viscoelastic dampers. In *Engineering Structures*, 3rd ed.; Elsevier: Amsterdam, The Netherlands, 2006; pp. 1197–1208. [CrossRef]
34. Yamaguchi, H.; Zhang, X.-R.; Niu, X.-D.; Nishioka, K. Investigation of Impulse Response of an ER Fluid Viscous Damper. *J. Intell. Mater. Syst. Struct.* **2010**, *21*, 423–435. [CrossRef]
35. Hou, C.-Y. Fluid Dynamics and Behavior of Nonlinear Viscous Fluid Dampers. *J. Struct. Eng.* **2008**, *134*, 56–63. [CrossRef]
36. Kabiri Rahani, E.; Bakhshi, A.; Golafshani, A.A. Semiactive Viscous Tensile Bracing System. *J. Struct. Eng.* **2009**, *135*, 425–436. [CrossRef]
37. Shi, M.; Fu, W.; Li, M.; Wang, H. Performance Test and Finite Element Modeling of Variable Damping Viscous Damper. *Soil Dyn. Earthq. Eng.* **2024**, *184*, 108838. [CrossRef]
38. Fan, F.; Shen, S.Z.; Parke, G.A.R. Theoretical and Experimental Study of Vibration Reduction in Braced Domes Using a Viscous Damper System. *Int. J. Space Struct.* **2004**, *19*, 195–202. [CrossRef]
39. Whittle, J.; Williams, M.S.; Blakeborough, A. Preliminary Study of Optimal Placement of Viscous Dampers in Buildings. In Proceedings of the 9th U.S. National and 10th Canadian Conference on Earthquake Engineering, Toronto, ON, Canada, 25–29 July 2010.
40. Hejazi, F.; Farahpour, H.; Ayyash, N.; Chong, T. Development of a Volumetric Compression Restrainer for Structures Subjected to Vibration. *J. Build. Eng.* **2022**, *46*, 103735. [CrossRef]